Contents lists available at ScienceDirect

Icarus
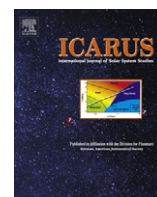
Rheological structure of the mantle of a super-Earth: Some insights from mineral physics

Shun-ichiro Karato

Yale University, Department of Geology & Geophysics, New Haven, CT 06520, USA

ABSTRACT

The rheological properties of the mantle of super-Earths have important influences on their orbital and thermal evolution. Mineral physics observations are reviewed to obtain some insights into the rheological properties of deep mantles of these planets where pressure can be as high as ∼1 TPa. It is shown that, in contrast to a conventional view that the viscosity of a solid increases with pressure (at a fixed temperature), viscosity will decrease with pressure (and depth) when pressure exceeds ∼0.1 TPa. The causes for pressure-weakening include: (i) the transition in diffusion mechanisms from vacancy to interstitial mechanism (at ∼0.1 TPa), (ii) the phase transition in MgO from B1 to B2 structure (at ∼0.5 TPa), (iii) the dissociation of $MgSiO_3$ into MgO and SiO_2 (at ∼1 TPa), and (iv) the transition to the metallic state (at ∼1 TPa). Some (or all) of them individually or in combination reduce the effective viscosity of constituent materials in the deep interior of super-Earths. Taken together, super-Earths are likely to have low viscosity deep mantle by at least 2–3 orders of magnitude less than the maximum viscosity in the lower mantle of Earth. Because viscosity likely decreases with pressure above ∼0.1 TPa (in addition to higher temperatures for larger planets), deep mantle viscosity of super-Earths will decrease with increasing planetary mass. The inferred low viscosity of the deep mantle results in high tidal dissipation and resultant rapid orbital evolution, and affects thermal history and hence generation of the magnetic field and the style of mantle convection.

© 2010 Elsevier Inc. All rights reserved.

1. Introduction

Recently more than 400 of exo-planets have been found making the list of planets much richer than we had before (e.g., http://exo-planets.org, Howard et al., 2010). These exo-planets include planets with the mass exceeding Earth mass, $M_\oplus$, but less than that of giant planets, called super-Earths. Super-Earths may have a range of compositions (Valencia et al., 2007a), but mantles of these planets are likely made of silicates or oxides much the same as Earth. With increasing number of observed super-Earths, several groups of scientists initiated a series of studies to develop models of structure and evolution of Earth-like planets in general (Papuc and Davies, 2008; Sotin et al., 2007; Valencia and O'Connell, 2009; Valencia et al., 2006, 2007a,b). In most of them, compositional models of these planets are discussed, but there were no previous studies on the rheological properties of super-Earths in any detail.

Rheological properties have strong influence on the nature of mantle convection that controls most of the dynamics and evolution of terrestrial planets (Schubert et al., 2001). Rheological properties also control tidal dissipation that will affect the temperature and orbital evolution of planets (Goldreich and Soter, 1966; Peale

and Cassen, 1978; Valencia and O'Connell, 2009; Valencia et al., 2007b). Viscosity of any condensed materials depends both on temperature and pressure (e.g., Karato, 2008). However, the influence of pressure dependence of viscosity was not investigated in any detail in the previous studies on super-Earths. For instance, (Valencia and O'Connell, 2009) did not consider the influence of pressure on viscosity in their analysis of viscosity of super-Earth. In recent papers by Papuc and Davies (2008) and Tachinami et al. (2010), some discussions are presented on the influence of total mass on the rate of mantle convection and other processes of super-Earths. Papuc and Davies (2008) and Tachinami et al. (2010) adopted a simple relationship between pressure and viscosity where $\log \eta$ (η: viscosity) increases linearly with pressure,

$$\log \eta = a + bP \tag{1}$$

where a and b are constants ($b = \frac{V^*}{RT} > 0$, V^*: activation volume, P: pressure), and concluded that a super-Earth with a larger mass will have a larger average viscosity.

The assumption of monotonic increase in viscosity with pressure at a constant temperature used by Papuc and Davies (2008) and Tachinami et al. (2010) is based on the limited knowledge at relatively low pressures that viscosity of most of solids increases with pressure (e.g., Karato, 2008). However, the limitation of such a model becomes obvious if one considers rheological properties of

E-mail address: Shun-ichiro.karato@yale.edu

matter at a very high degree of compression. When a material such as FeO is compressed to a large degree, electron orbits start to overlap leading to the metallic state (e.g., Mott, 1968) and further compression leads all materials to a dense state, $\rho > \frac{m^{5/2}}{h^3}(2\pi k_B T)^{3/2}$ (ρ: density, m: atomic mass, h: the Planck constant, k_B the Boltzmann constant, T: temperature), where the mean distance of atoms becomes smaller than the de Broglie length. In such a case, the quantum mechanical tunneling effects allow nearly free relative motion of atoms leading to a low viscosity (e.g., Landau and Lifshitz, 1964). Therefore if viscosity increases with pressure at low pressures, there must be some critical pressure above which viscosity of a given material decreases with pressure.

In this paper, I will examine plausible mechanisms to cause such a change in the viscosity–pressure relationship. Because direct experimental studies under these conditions are missing, one cannot obtain any detailed quantitative results, but limitations with conventional approaches can be identified that will help guide studies in this area. It will be shown that the conventional idea of increase of viscosity with depth is not valid at pressures comparable to or exceeding the zero-pressure bulk modulus of the material ($P/K_0 > 1$, P: pressure, K_0: bulk modulus (at $P = 0$)), and that there will be a maximum in viscosity at a certain pressure on the order of $P/K_0 \approx 1$ (~0.1 TPa for most of oxides and silicates). Consequently, the viscosity of the deep interior of super-Earths will be smaller as the total mass of a planet increases. Some consequence of such a rheological structure on the dynamics and evolution of super-Earths will also be discussed.

2. Structure of a super-Earth

2.1. Pressure and temperature in super-Earths

Sotin et al. (2007) and Valencia et al. (2006, 2007b) investigated the structure of super-Earths. The pressure–depth relationships for these planets can be developed based on the assumption of hydrostatic equilibrium, and the pressure is found to be ~1 TPa at the based of mantle of the super-Earth with a total mass of 7 $M_\oplus$ (Sotin et al., 2007). Temperature distribution is uncertain because both the distribution of heat sources and the rate of heat transport by convection are not well known. Consequently, although the temperature gradient in the main portion of mantles of super-Earths is reasonably well constrained by the adiabatic gradient, the absolute value of temperature is highly uncertain.

In this paper, I will first use the temperature–depth profile for 7 $M_\oplus$ super-Earth estimated by Sotin et al. (2007) and Valencia et al. (2006) to examine the general trend in the rheological behavior of mantle materials in the pressure range of ~0.1 to ~1 TPa. Such a discussion provides a guide as to the possible rheological behaviors in this pressure range. However, results for a given temperature profile cannot be extended to investigate the influence of planetary mass on the (average) viscosity because of the important role of temperature–viscosity feedback. The influence of temperature–viscosity feedback will be discussed later after I discuss a plausible range of rheological behavior, and the viscosity–mass relationships for super-Earths will be examined and its implications for the evolution of super-Earths will be discussed.

2.2. Materials in super-Earths

In this paper, I will consider super-Earths with Earth-like compositions. A standard compositional model of Earth is the pyrolite model (Ringwood, 1975) that is made of a mixture of many oxides and silicates (mostly MgO, FeO, SiO$_2$, CaO, Al$_2$O$_3$ and their compounds). However, because the purpose of this paper is to examine the gross rheological behavior of such planets, I choose a simple

compositional model where the mantle is made of MgO and MgSiO$_3$. In this model, the majority of mantles of super-Earths will be made of perovskite (MgSiO$_3$) + MgO (0.024 TPa < P < 0.12 TPa), post-perovskite (MgSiO$_3$) + MgO (at P > 0.12 TPa) and finally a mixture of MgO + SiO$_2$ (at P > 1 TPa, Umemoto et al., 2006). MgO undergoes a phase transition from NaCl (B1) to CsCl (B2) structure at $P \sim 0.5$ TPa (Karki et al., 1997; Oganov et al., 2003) (Fig. 2) (these are essentially pressure-induced phase transitions and the influence of temperature is minor (for $T \sim 5000$ K, $\Delta P \approx 0.01$–0.03 TPa)). It is also noted that some of these oxides may change into the metallic state under those conditions (e.g., Gramsch et al., 2003; Mott, 1968; Nellis, 2010; Umemoto et al., 2006).

3. Rheological properties under high pressure, temperature conditions

3.1. General introduction

Viscous deformation of solids occur through a variety of mechanisms (e.g., Frost and Ashby, 1982; Karato, 2008). At typical conditions in the deep mantle, i.e., relatively high homologous temperatures ($T/T_m > 0.5$, T_m: melting temperature) and low stresses ($\sigma/\mu < 10^{-3}$, σ: stress, μ: shear modulus), most of solids deform plastically by mechanisms involving thermally activated motion of crystalline defects. In these cases, the viscosity of solids depends strongly on temperature and pressure as,

$$\eta = \eta_0 \exp\left(\frac{H^*(P) - H^*(P_0)}{RT}\right) \qquad (2a)$$

where η is the viscosity at pressure P, η_0 is a reference viscosity (at pressure P_0), $H^*(P)$ is the activation enthalpy at pressure P, and R is the gas constant. In many cases, the rate-controlling process of deformation includes diffusion of atoms, and I will use a simple diffusion-controlled model of high-temperature deformation where the activation enthalpy of deformation is the same as that of diffusion (of the slowest diffusing species) (e.g., Karato, 2008).

The pre-exponential factor may also depend on pressure, and in such a case, Eq. (2a) needs to be modified to,

$$\eta = \eta_0 \left(\frac{X(P)}{X(P_0)}\right) \exp\left(\frac{H^*(P) - H^*(P_0)}{RT}\right) \qquad (2b)$$

where $X(P)$ is an pre-exponential factor. However, the pre-exponential term changes with pressures only modestly compared to a possible range of change in $\exp\left(\frac{H^*(P)-H^*(P_0)}{RT}\right)$ term. For instance, if one assumes $H^* = E^* + PV^*$ with $V^* = 10 \times 10^{-6}$ m^3/mol, then for a
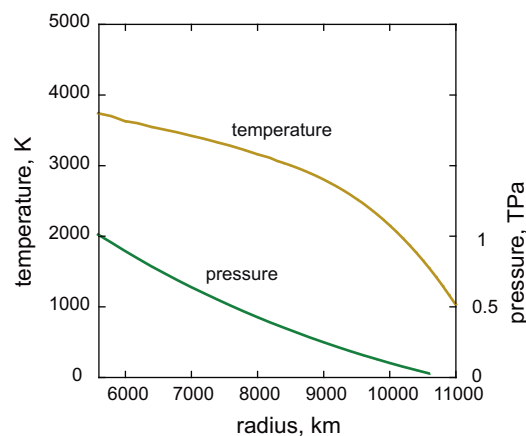

Fig. 1. The pressure–temperature distribution of the mantle of a super-Earth with a mass of 7 $M_\oplus$ (after Valencia et al. (2006)).
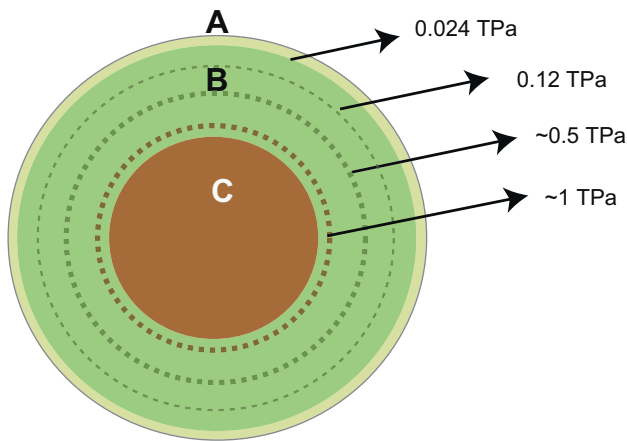
Fig. 2. A schematic model of the structure of a super-Earth (a super-Earth with Earth-like composition with a mass of 7 $M_\oplus$) (from Valencia et al. (2007b)). The radius is ~11,000 km, A: upper mantle (olivine-rich), B: lower mantle (perovskite + MgO, post-perovskite + MgO, MgO + SiO₂), C: core. The core–mantle pressure is ~1.1 TPa and temperature is ~4000 K. The transition from upper to lower mantle is at ~0.024 TPa. MgO undergoes a phase transformation from the B1 (NaCl) to (B2) structure at ~0.5 GPa. MgSiO₃ perovskite changes to post-perovskite at ~0.12 TPa, and post-perovskite dissociates to MgO and SiO₂ at ~1 TPa. Metallization of oxides may occur at ~1 TPa or higher pressures.

typical mantle temperature of $T = 5000$ K and for a variation of $P - P_0 = 1$ TPa, $\frac{\eta}{\eta_0} \approx 10^{100}$, while the change in the pre-exponential term is about a factor of ~10 (I used a model where the pre-exponential term is made primarily of the Debye frequency). Therefore I will focus on the exponential term in this paper. When crystal structure changes or the nature of chemical bonding changes, then all terms may change. In these cases, I will use a more general approach using the systematics in high-temperature rheological properties.

Note also that parameters such as η_0 and H^* depend on the material (crystal structure for a given composition) and on the mechanism of deformation both of which will change under high-pressure conditions in the deep interior of a super-Earth. Because the pressure in a super-Earth covers a broad range (to ~1 TPa ($P/K_0 \approx 10$)), all of these factors will play an important role in controlling the rheological properties. In the following sections, I will examine the influence of these factors separately.

3.2. Influence of pressure on viscosity

3.2.1. Pressure effects for a fixed deformation mechanism

Let us first consider a simple case where crystal structure and deformation mechanism remain the same. In such a case, the depth variation of viscosity is determined by the depth variation of $\frac{H^*(z)}{RT(z)}$. To examine how this term affects the viscosity–depth profile, I will use the temperature profile for a 7 $M_\oplus$ super-Earth calculated by Valencia et al. (2006). Because there are no experimental studies on viscosity under these conditions, I will use a semi-empirical approach to estimate the depth variation of viscosity through the calculation of $\frac{H^*(z)}{RT(z)}$. Widely used semi-empirical models for diffusion-related properties are (i) the homologous temperature scaling model (Sherby et al., 1970) and (ii) the elastic strain energy model (Keyes, 1963) for thermally activated processes (see Chapter 10 of Karato (2008)). In the homologous temperature scaling, activation energy is assumed to be proportional to the melting temperature, viz., $\frac{H^*(z)}{RT(z)} \propto \frac{T_m(z)}{T(z)}$. Therefore one needs to estimate the pressure (depth) dependence of melting temperature. However, these two methods are equivalent if one accepts the Lindemann model for melting and the Debye model of lattice vibration (Poirier and Liebermann, 1984).

Consequently, I will use the elastic strain energy model in this paper. The validity of the strain energy model was examined by Karato (1981) and Sammis et al. (1981). Karato (1981) showed that this model works well for migration enthalpy but not for formation enthalpy of defects (see also Chapter 10 of Karato (2008)). With this model, the activation enthalpy can be written as

$$H^*(z) = B \cdot C(z) \cdot V(z) \tag{3}$$

where B is a non-dimensional constant (on the order of ~0.1), C is a relevant elastic constant and V is the molar volume. This model provides an explanation for the decrease of activation volume with pressure (e.g., Poirier and Liebermann, 1984). Fig. 3 shows the variation of viscosity with depth (pressure) for MgO based on the results on elastic constants and molar volume from Karki et al. (1997). The temperature and pressure distribution corresponding to a super-Earth with 7 $M_\oplus$ shown in Fig. 1 are used. Similar results are obtained for perovskite (not shown). The depth variation of $H^*(z) = B \cdot C(z) \cdot V(z)$ depends strongly on the choice of C. Assuming, for simplicity, that C is a linear combination of bulk and shear moduli, i.e., $C = \phi K + (1 - \phi)G$ (K: bulk modulus, G: shear modulus), I calculated the results for a range of ϕ. It is seen that for a large value of ϕ, viscosity increases significantly with depth, but for a small value of ϕ, viscosity changes only slightly with depth. A value of ϕ consistent with the experimental data of activation energy and volume in MgO by Van Orman et al. (2003) is $\phi = 0.0$–0.2 yielding a viscosity–depth profile where viscosity is nearly independent of depth.

A similar conclusion was obtained by Yamazaki and Karato (2001) who calculated the viscosity–depth profiles of the Earth's lower mantle based on the experimental data on the activation energies and volumes of diffusion in MgO and MgSiO₃ perovskite.

3.2.2. Effects of a change in diffusion mechanism

In the above analysis, I assumed that the mechanism of diffusion remains the same, i.e., the values of B and ϕ do not change with pressure. However, in a broad range of pressures (and temperatures), microscopic processes of diffusion may change. Here I will examine a possible change in diffusion mechanism with pressure.

In a dense oxide such as MgO, diffusion of atoms at low pressures occurs mostly through the vacancy mechanism including the diffusion of a vacancy pair (e.g., Ando, 1989). However, the
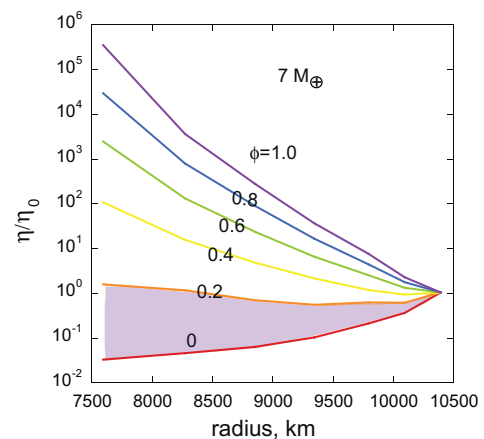

Fig. 3. The viscosity–depth profile corresponding to a case without phase transformation nor mechanism change. Viscosity–depth profile is calculated using Eq. (2) with an activation energy described by the strain energy model (Eq. (4)). Molar volume and elastic constants are from Karki et al. (1997) (the data on MgO are extended to higher pressures; personal communication with Bijay Karki). ϕ is a fraction of strain energy partitioned to the volumetric strain. The temperature-, and pressure–depth relations for the 7 $M_\oplus$ super-Earth are used (see Fig. 1a). Results for various models with $C = \phi K + (1 - \phi)G$ ($0 \leqslant \phi \leqslant 1$) are shown. Experimental observations for MgO (and perovskite) suggest $0 \leqslant \phi \leqslant 0.2$.

vacancy mechanism of diffusion may become inefficient at high pressures compared to the interstitial mechanism because the activation volume for the vacancy mechanism is larger than that for the interstitial mechanism. For simplicity, let us use a linear expression for activation enthalpy, i.e., $H_{1,2}^* = E_{1,2}^* + PV_{1,2}^*$, where $H_{1,2}^*$ is the activation enthalpy, $E_{1,2}^*$ is the activation energy, and $V_{1,2}^*$ is the activation volume for mechanism 1, 2 respectively. At low pressures, a mechanism with a smaller activation energy will dominate, whereas, at high pressures, the influence of activation volume becomes important and a mechanism with a lower activation volume will dominate (i.e., for MgO $E_1^* > E_2^*$ and $V_2^* > V_1^*$, 1: interstitial mechanism and 2: vacancy mechanism). The transition pressure is given by

$$P = \frac{E_2^* - E_1^*}{V_1^* - V_2^*} \qquad (4)$$

where I assumed that the difference in activation entropy (the pre-exponential term) is small ($\exp(\frac{S^*}{R}) \approx 1$, see Shewmon, 1989). If such a transition occurs, then activation volume decreases and the viscosity in the high-pressure region will be lower than expected for a case of no transition in diffusion mechanism.

This model was studied by Karato (1978) for a simple case of a mono-atomic *fcc* crystal based on the theoretical calculation of defect energies using a method by Kanzaki (1957) (for a brief summary see Appendix A). Results supporting such a concept was recently published by Ito and Toriumi (2007) who made molecular dynamics calculations of diffusion in MgO. They showed that the viscosity calculated from diffusion coefficient in MgO has the maximum at ∼60 GPa (∼0.4 *Ko*) after which it decreases with pressure (Fig. 4). Although the atomistic mechanism to cause the minimum of diffusion coefficients was not investigated by Ito and Toriumi (2007), it is possible that this is caused by the transition from the vacancy to interstitial mechanism of diffusion. If this phenomenon occurs in the planetary mantle, then viscosity will be lower than expected from a case without mechanism transition. Note that the viscosity maximum (the diffusion minimum) was not observed in other numerical studies where the diffusion mechanism was assumed to be vacancy mechanism and the possibility of the mechanism change was not considered (e.g., Ita and Cohen, 1997).

However, Karato (1978) also found that this mechanism transition is highly sensitive to the nature of inter-atomic potential, and the transition pressure increases strongly with the increase in the "stiffness" of the potential. When the potential is stiff, formation of an interstitial atom needs a large amount of energy, and hence the
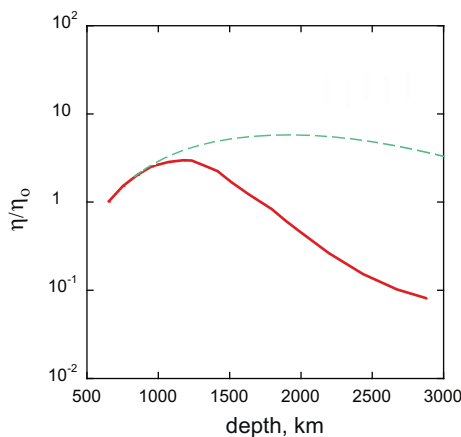
transition pressure from the vacancy to the interstitial mechanism becomes high. Therefore the transition pressure is likely sensitive to materials. Based on the results by Ito and Toriumi (2007) and Karato (1978), I assume that this transition occurs in MgO at ∼0.1 TPa. After such a transition, viscosity will become lower than the case without a mechanism change and the degree of viscosity reduction is larger at higher pressures.

3.3. Influence of phase transformations

Phase transformations occur in most of mantle minerals under high-pressure conditions in a planet. Various factors can affect the rheological properties upon a phase transformation (for a review see Chapter 15 of Karato (2008)). The change in grain-size has the largest effect at low temperature, but the most important mechanism is the influence of the change in crystal structure under most of high-temperature conditions in the mantle of super-Earths. The influence of crystal structure can be studied through the studies on analog materials (e.g., Frost and Ashby, 1982; Karato, 1989). Fig. 5 provides such a result based on Karato (1989) and Frost and Ashby (1982). This figure indicates that among the possible constituent of the mantles of super-Earths, MgO (with the B1 (NaCl) structure) likely has the lowest viscosity and hence has an important role in controlling the average viscosity of the mantles of these planets (see also Yamazaki and Karato, 2001).

MgO likely changes its structure from B1 to B2 at ∼0.5 TPa. However, in the previous work by Karato (1989), creep strength of materials with B2 structure was not considered. Here, I examine the differences in high-temperature creep behavior in materials with these two structures. Two different data sets are available to compare the difference in viscosity between B1 and B2 structure. First is a comparison of high-temperature power-law creep behavior between NaCl (Franssen, 1994) and CsCl (Heard and Kirby, 1981) (Fig. 6a). Compared at the same normalized conditions, CsCl shows substantially smaller creep strength than NaCl (by a fac-

Fig. 4. Solid curve: the normalized viscosity (η: viscosity, η_0: viscosity at 660 km depth), as a function of depth in Earth's mantle based on the molecular dynamics calculations of diffusion coefficients in MgO by Ito and Toriumi (2007) showing the maximum at ∼1200 km (60 GPa (∼0.4 *Ko*)). Broken curve: a viscosity–depth profile without the change in activation volume (diffusion mechanism).
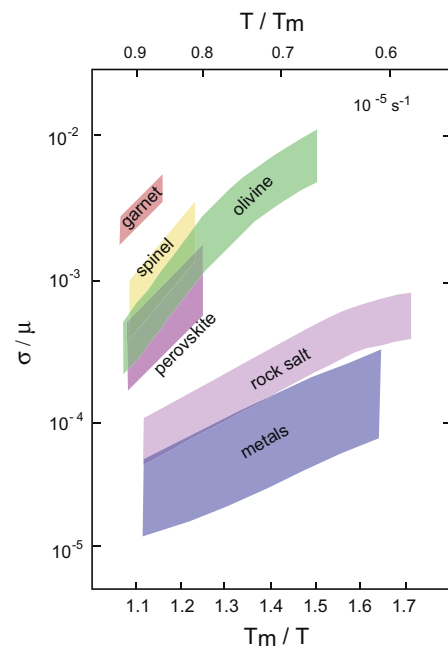

Fig. 5. The crystal structure versus creep strength systematics for various materials for power-law dislocation creep (based on Frost and Ashby (1982) and Karato (1989)). Normalized stress (σ/μ, σ: deviatoric stress, μ: shear modulus) is plotted against normalized temperature (T_m/T, T: temperature, T_m: melting temperature) for a strain-rate of 10^{-5} s^{-1}. The results for metals include those with *fcc*, *bcc* and *hcp* structures from Frost and Ashby (1982).

tor of $\sim$10–10^2). Under the conditions explored in these studies, both of these materials show power-law creep behavior with the stress exponent of n = 4.4, but the creep strength of CsCl is systematically smaller than that of NaCl (after the normalization).

A similar conclusion can be drawn from the comparison of energies of point defects (Rowell and Sanger, 1981) (Fig. 6b). Defect formation energies are much the same between these structures, whereas defect migration energies are distinctly different. Consequently, the viscosity ratio between materials with these structures was calculated using the defect migration energies,

$$\frac{\eta_{B1}}{\eta_{B2}} = \exp\left(\frac{G^*_{B1} - G^*_{B2}}{RT}\right) \qquad (5)$$

where $\eta_{B1,B2}$ is the viscosity of the B1 or B2 phase, and $G^*_{B1,B2}$ is the migration energy of point defects in the B1 or B2 phase respectively. From the data complied in Fig. 6b, I estimate the viscosity ratio is $\frac{\eta_{B1}}{\eta_{B2}} \sim 10^2$.

Similar results (smaller strength of the B2 phase than the B1 phase) were reported for low-temperature plasticity in MgO (Meade and Jeanloz, 1988), although these results are not applicable to deformation in planetary interiors. I conclude that materials with the B2 structure have considerably smaller creep strength than those of the B1 structure under most conditions. A comparison of diffusion coefficients of silicate perovskite and MgO also shows a result similar to those shown in Fig. 5: diffusion coefficients in perovskite are considerably smaller than those in MgO (Yamazaki and Karato, 2001).

Previous studies on deformation of post-perovskite phase have been focused on deformation microstructures (lattice-preferred
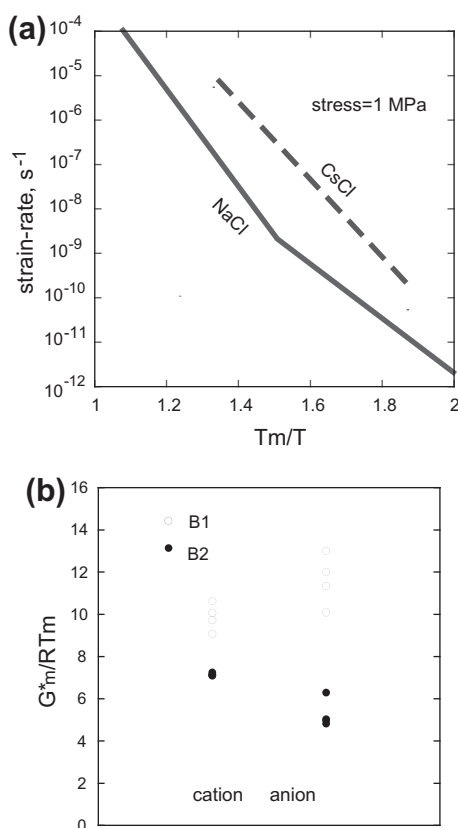
Fig. 6. A comparison of (a) high-temperature creep and (b) point defect migration energies between B1 and B2 structure. (a) A comparison of high-temperature creep in NaCl (Franssen, 1994) and CsCl (Heard and Kirby, 1981). (b) A comparison of energies of point defects in NaCl and CsCl (Rowell and Sanger, 1981). G^*_m is the migration energy of vacancy, T_m is the melting temperature.

orientation) (Merkel et al., 2007; Miyagi et al., 2008; Yamazaki et al., 2006) and no systematic studies have been made on high-temperature creep of materials with the CaIrO$_3$ structure (post-perovskite structure). The only published quantitative study on a post-perovskite phase that is related to high-temperature creep is a paper by Ammann et al. (2010). They calculated defect migration energies in the post-perovskite phase of MgSiO$_3$ and other co-existing minerals under the D'' layer conditions (0.13 TPa), and found large anisotropy in defect migration energy in the post-perivskite. However, defect concentration was not calculated and therefore no quantitative conclusions on diffusion (and hence diffusion-controlled high-temperature creep) can be obtained from this study. If one makes an assumption (as these authors did) that the defect concentrations are the same among co-existing minerals and takes an appropriate average of diffusion coefficient, then one would conclude that the post-perovskite phase has a similar or somewhat larger creep strength (viscosity) than perovskite and much stronger than (Mg, Fe)O (this conclusion is different from the conclusion by Ammann et al. (2010) because they used an incorrect averaging scheme as discussed by Karato (2010)).

3.4. Influence of metallization

As pressure increases, the inter-atomic distance is reduced and then electron orbits (wave functions of electrons) of neighboring ions overlap more and more. Consequently, at a certain point the outer electrons of ions will be delocalized and hence the material becomes metallic (e.g., Mott, 1968). Transition to metallic state in some oxides has been reported (e.g., Knittle and Jeanloz, 1986; Todo et al., 2001). Although there is no convincing case for metallization of Earth-like oxides (such as (Mg,Fe)O), it is theoretically feasible that metallization occurs eventually as one squeezes an oxide (transition may occur at around $\sim$1 TPa for some oxides, see Umemoto et al., 2006). As seen from Fig. 5, metals in general have smaller viscosity than other oxides compared at the same normalized conditions and therefore this possible metallization will reduce the creep strength (viscosity) (oxides with the B2 structure may be an exception: they may be as weak as metals).

4. Models of rheological structure of super-Earths

4.1. A model of viscosity–depth profile for a fixed temperature–depth profile

In super-Earths with Earth-like composition, a majority of the mantle is made of lower mantle type materials (Valencia et al., 2007a). In the simple model used in this paper, the constituent minerals of super-Earths are perovskite (MgSiO$_3$) + MgO, post-perovskite (MgSiO$_3$) + MgO and MgO + SiO$_2$. I will discuss the rheological properties of such a region of super-Earths. In all of these regions, relatively weak MgO occupies $\sim$20–30% (in perovskite + MgO, post-perovskite + MgO) to $\sim$60% (in MgO + SiO$_2$). With an inferred rheological contrast between MgO and co-existing phases, a volume fraction of $\sim$20–30% exceeds the percolation threshold, and the rheological properties of a mixture are largely controlled by that of a weak phase (IWL model by Handy (1994), see also Stauffer and Aharony, 1992).

Given such a model, one can recognize four processes that will affect the rheological properties substantially:

mechanism I ($\sim$0.1 TPa): transition in diffusion mechanism,
mechanism II ($\sim$0.5 TPa): B1 → B2 transition in MgO,
mechanism III ($\sim$1 TPa): dissociation of post-perovskite into oxides,
mechanism IV ($\sim$1 TPa or higher): metallization of oxides.

The magnitude of viscosity reduction at each step is not well constrained by currently available data but using the systematics and semi-quantitative study, one can make some plausible estimates. The viscosity reduction by the mechanism I is gradual but can be large (see Fig. 7). The mechanism II will further reduce the viscosity by a factor of $\sim 10^2$ (see Fig. 6). The mechanism III will further reduce the viscosity by a factor of ~ 3 through the increase in the volume fraction of a weaker phase MgO (from 20–30% to ~ 50–60%). Metallization (mechanism IV) will also reduce the viscosity. Although the dissociation of post-perovskite and metallization have not been well established, all of these processes lead to rheological weakening.

Consequently, I conclude that the viscosity of mantle materials at a given temperature is likely reduced by the increase of pressure in the pressure range exceeding ~ 0.1 GPa. The magnitude of decrease in viscosity is difficult to estimate, but using the above estimated values and assuming a simple adiabatic temperature profile, I conclude that the overall reduction in viscosity is at least by two to three orders of magnitude. If an analogy to Earth's mantle is made and the average (peak) viscosity of $\sim 10^{22}$ Pa s for the lower mantle of Earth is used as a representative viscosity before the above mentioned processes take in (at ~ 0.1 TPa), then the viscosity of the deep mantles of super-Earths is estimated to be on the order of $\sim 10^{19}$ Pa s for a super-Earth with 7 $M_\oplus$ (Fig. 7). Because the viscosity maximum occurs at ~ 0.1 GPa or so, the critical mass above which deep mantle viscosity starts to decrease with mass is ~ 1 $M_\oplus$.

4.2. Influence of viscosity–temperature feedback

In the previous sections, possible factors controlling the rheological properties of super-Earths' mantle were discussed for an assumed temperature–depth profile. However, temperatures in a planet are strongly controlled by the rheological properties and consequently, in a more complete study, the viscosity–temperature feedback needs to be included through a self-consistent
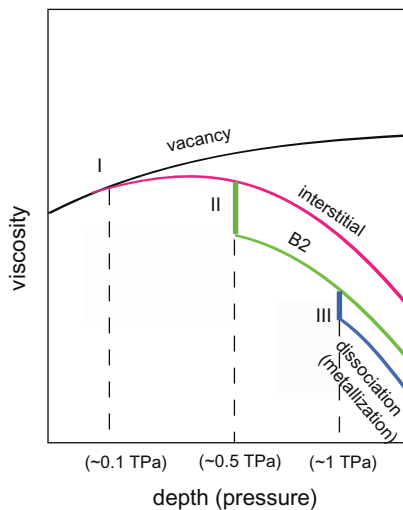

Fig. 7. A schematic diagram showing the influence of various processes to modify the viscosity–depth relationship. The following three processes are considered: I: influence of mechanisms change in diffusion (~ 0.1 TPa). II: influence of B1–B2 transition in MgO (~ 0.5 TPa). III: influence of dissociation of MgSiO (~ 1 TPa). A broken curve represents the viscosity–depth profile without these processes. The variation of viscosity by a process I is continuous and its magnitude becomes larger as pressure increases. The variation of viscosity by a process II is about two orders of magnitude (from Fig. 6). The reduction of viscosity by a process III is a factor of ~ 3 (caused by the increase in the volume fraction of MgO from ~ 20–30% to ~ 50–60%). Metallization of oxides may occur at ~ 1 TPa or higher pressures that will also reduce the viscosity.

analysis (e.g., Tozer, 1972). This is critical particularly when one compares the viscosity profiles of planets with different masses. An analysis of such a feedback will involve the calculation of thermal history (e.g., Kite et al., 2009; Papuc and Davies, 2008; Tachinami et al., 2010). However, for simplicity, I will analyze the effect of this feedback for the steady-state where heat generation is balanced with heat loss, viz.,

$$M.H = A \cdot Nu \cdot k \frac{T - T_s}{d} \tag{6}$$

where M is the mass of the planet, H is heat production per unit mass (by radioactive elements), A is the total surface area, Nu is the Nusselt number, k is thermal conductivity, T is the representative temperature (the potential temperature), T_s is the surface temperature, and d is the thickness of the mantle. The Nusselt number represents the rate of heat transfer by convection relative to the conductive heat transfer and hence depends on the viscosity, viz.,

$$Nu = \left(\frac{\rho g \alpha (T - T_s) d^3}{\kappa \eta} \right)^\beta \tag{7}$$

where β is a non-dimensional constant ($\sim 1/3$ for a simple boundary layer model of convection; Schubert et al., 2001), g is the acceleration due to gravity, α is thermal expansion, ρ is density and K is thermal diffusivity ($\kappa = \frac{k}{\rho C_p}$, C_p: specific heat). If one assumes that the Nusselt number depends on the representative temperature (viscosity) of the mantle (the parameterized convection approach, Schubert et al., 2001), then Eq. (6) provides a relationship between mantle temperature and mass relationship.

In some previous studies on super-Earth, a power-law relationship between some properties and the planetary mass was explored (e.g., Valencia and O'Connell, 2009; Valencia et al., 2007b). In order to facilitate a comparison to these studies, I use the following simple form of temperature and pressure dependence of viscosity,

$$\eta \propto T^{-\theta} P^\psi \tag{8}$$

where θ and ψ are non-dimensional parameters that characterize the temperature and pressure dependence of viscosity respectively. If one uses the Arrhenius relation, $\eta \propto \exp\left(\frac{E^* + PV^*}{RT}\right)$, with a constant V^*, then $\theta = \frac{E^* + PV^*}{RT}$ and $\psi = \frac{PV^*}{RT}$. Obviously, neither θ nor ψ is truly constant but they depend on temperature and pressure. However, when the temperature and pressure range are small, this parameterization can be justified as a crude guide to investigate the relation between planetary mass and temperature (and viscosity).

In the following, I will consider a simple case of constant density, thermal expansion, thermal diffusivity, and I will also assume $T \gg T_s$. This simplification may be justified because the variation of thermal expansion, density and thermal conductivity is much smaller than the possible range of variation of viscosity. Given these assumptions, $P \propto M^{2/3}$ and one has

$$T \propto M^{\frac{2(1-2\beta+\psi\beta)}{3(1+\beta+\theta\beta)}} \left(= M^{\frac{2(1+\psi)}{3(4+\theta)}} \quad \text{for } \beta = \frac{1}{3} \right) \tag{9}$$

and

$$\eta \propto M^{-\frac{2(1-2\beta+\psi\beta)\theta}{3(1+\beta+\theta\beta)} + \frac{2}{3}\psi} \left(= M^{-\frac{2(\theta-4\psi)}{3(4+\theta)}} \quad \text{for } \beta = \frac{1}{3} \right) \tag{10}$$

$\frac{d\log T}{d\log M}$ and $\frac{d\log\eta}{d\log M}$ calculated from Eqs. (9) and (10) are plotted as a function of θ and ψ in Fig. 8. When viscosity is independent of temperature and pressure, then $\frac{d\log T}{d\log M} = 0.17$ and $\frac{d\log T}{d\log M} = 0$. When viscosity is sensitive to temperature but not to pressure, then $\frac{d\log T}{d\log M} \approx 0.02$ and $\frac{d\log\eta}{d\log M} \approx -0.6$ for $\theta = 30$ and $\psi = 0$ for example (see also Fig. 8). Due to the self-regulation effects by the viscosity–temperature
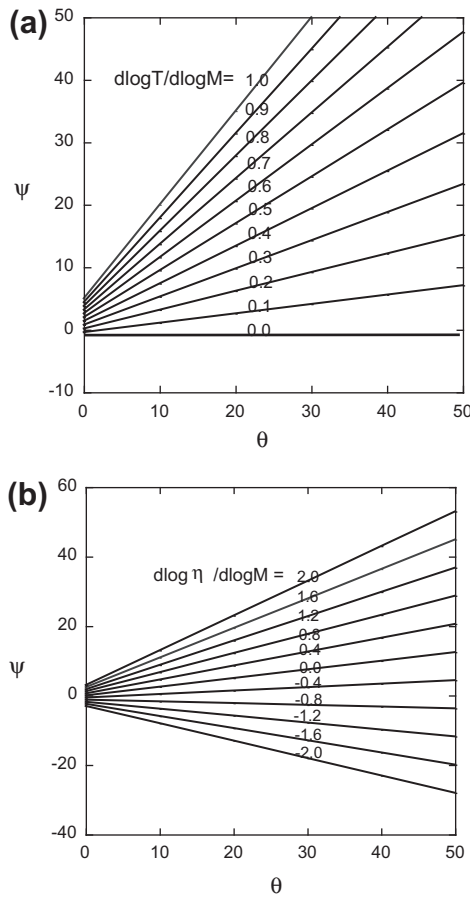
Fig. 8. Values of $\frac{d\log T}{d\log M}$ and $\frac{d\log\eta}{d\log M}$ as a function of two parameters (θ, ψ) characterizing the temperature and pressure dependence of viscosity, $\eta \propto T^{-\theta}P^{\psi}$.

feedback, temperature in a planet is relatively insensitive to the mass, but viscosity decreases with the mass. When pressure effect is introduced, these trends change drastically. For instance, if $V^* = 3 \times 10^{-6}$ m³/mol (with $E^* = 300$ kJ/mol), then $\frac{d\log T}{d\log M} \approx 0.8$ and $\frac{d\log\eta}{d\log M} \approx 2$ ($\theta \approx 40$ and $\psi \approx 40$). In such a case, viscosity increases strongly with the planetary mass despite the increase in temperature, and convection becomes sluggish in a large planet. However, if the viscosity decreases with pressure as I suggest in this paper, then the dependence of viscosity on planetary mass will be different. In these cases, the temperature–pressure dependence of viscosity becomes complicated and θ and ψ need to be interpreted as effective parameters. For instance, if the pressure dependence of viscosity becomes negative due to the influence of the mechanism change as discussed in Appendix, then the pressure dependence is negative although the activation enthalpy remains positive. In terms of effective parameters, such a situation corresponds to $\theta > 0$ and $\psi < 0$, and hence viscosity decreases with planetary mass, $\frac{d\log\eta}{d\log M} < 0$.

5. Discussion

5.1. Implications for tidal dissipation

The proposed low viscosity of the deep mantles of super-Earths has a direct implication for tidal dissipation. Tidal dissipation due to non-elastic deformation caused by the interaction of a super-Earth with its parent star controls the orbital evolution of a super-Earth (e.g., Lin et al., 1996). Tidal dissipation occurs through-

out the planet, but most of tidal energy is stored in the deep part of the mantle (Peale and Cassen, 1978). Consequently, the results of present study on deep mantle viscosity can be applied directly to tidal dissipation.

If we assume Maxwell body behavior, then the energy dissipation by tidal dissipation, $\dot{E}(\tau)$, is proportional to $\frac{\omega\tau}{1+\omega^2\tau^2}$ (ω: frequency of tidal deformation, $\tau\left(=\frac{\eta}{\mu}\right)$ is the Maxwell time (μ: shear modulus, η: viscosity of the deep mantle)) and $\frac{\dot{E}(\tau)}{\dot{E}_{max}} = \frac{2\omega\tau}{1+\omega^2\tau^2}$ with ($\dot{E}_{max}$: the maximum energy dissipation as a function of relaxation time) (e.g., Ross and Schubert, 1986). For a typical frequency of $\omega \approx 10^{-6}$ s^{-1}, elastic modulus of $\mu \approx 10^{12}$ Pa, and a viscosity of $\eta \approx 10^{22}$ Pa s (typical lower mantle viscosity in Earth's lower mantle), we get $\frac{\dot{E}(\tau)}{\dot{E}_{max}} \approx 2 \times 10^{-4}$. However, if a lower viscosity, say $\eta \approx 10^{19}$ Pa s is used as discussed in this paper then one gets much more intense tidal dissipation, $\frac{\dot{E}(\tau)}{\dot{E}_{max}} \approx 2 \times 10^{-1}$. High tidal dissipation results in large internal heating and further reduces viscosity that in turn enhances orbital evolution. The orbital evolution of these super-Earths would be faster than previously thought.

5.2. Implications for thermal evolution, plate tectonics and magnetic field generation

A number of important processes on a planet including volcanic activities, generation of magnetic field, and the style of mantle convection (e.g., plate tectonics versus stagnant-lid convection) depend strongly on the rheological properties of its mantle. Several previous studies addressed the nature of these activities on super-Earths with a different degree of complications (e.g., Gaidos et al., 2010; Kite et al., 2009; Papuc and Davies, 2008; Tachinami et al., 2010; Valencia and O'Connell, 2009). For instance, Tachinami et al. (2010) and Gaidos et al. (2010) evaluated the conditions for magnetic field generation. When magnetic field is generated in the core by dynamo, the conditions for magnetic field generation is that the core is cooled rapidly enough to allow vigorous convection (e.g., Gaidos et al., 2010; Tachinami et al., 2010). Consequently, the issue of generation of magnetic field on a planet is boiled down to the evaluation of the rate of heat transport in the mantle, which depends on mantle viscosity. When the conditions for the operation of plate tectonics are examined, one compares the stress magnitude on the plate caused by convection with the resistance force for plate subduction, and when the former is larger than the latter, the surface layer can subduct and plate tectonics would occur (e.g., O'Neill et al., 2007; Valencia and O'Connell, 2009).

In these studies, one of the goals is to evaluate the conditions where certain geodynamic activities operate on super-Earths as a function of planetary mass. Consequently, the use of a proper scaling relationship between the planetary mass and viscosity is essential. However, due to the lack of understanding of the influence of pressure on viscosity under high-pressure conditions relevant to super-Earths, either pressure dependence of viscosity was ignored (Valencia and O'Connell, 2009) or a conventional formula such as $\eta = \eta_0 \exp\left(\frac{E^*+PV^*}{RT}\right)$ with a constant V^* was used (Papuc and Davies, 2008; Tachinami et al., 2010) in the previous studies. The use of a different scaling relationship proposed here will have an important impact on the studies of dynamic activities on super-Earths.

6. Summary and perspectives

As a large number of Earth-like planets are found at various distances from their parent stars, it is important to understand the dynamics and evolution of these planets including their orbital evolution and some tectonic activities such as the presence or the absence of plate tectonics and the magnetic field. The rheological properties of their mantles are among the key properties that have an important control on these issues.

Materials science observations are reviewed to obtain some insights into these properties in the deep mantle of super-Earths. Four processes are identified that may have important influence on rheological properties of rocky materials under 1 TPa range pressures. They include (i) a change in diffusion mechanism (at ~0.1 TPa), (ii) the B1 to B2 phase transition in MgO (at ~0.5 TPa), (iii) the dissociation of MgSiO₃ post-perovskite (~1 TPa), and (iv) the possible metallization of oxides (~1 TPa or higher). All of them reduce the viscosity of these materials. However, currently quantitative studies on the influence of these processes on rheological properties are lacking. The presence of the minimum diffusion coefficient has not been confirmed by experiments, and not many data exist to demonstrate a large rheological contrast between the materials with the B1 and B2 structure. Predicted dissociation of the post-perovskite phase of MgSiO₃ has not been confirmed (an experimental study on the analog material, NaMgF₃ by Grocholski et al. (2010) did not show the dissociation at ~40 GPa predicted some theoretical calculations). I also note that possible phase transformations such as the B1 to B2 and the dissociation of post-perovskite also change the melting temperature, that in turn affect the rheological properties. Experimental tests or computational studies on these issues are important to make further progress in our understanding of the evolution and dynamics of these planets.

Appendix A. Transition in the dominant type of point defect under high-pressures

In any crystal, point defects are present at finite temperature. Several transport properties such as diffusion and creep involve motion of point defects, and the rate of these processes is proportional to the defect concentration and defect mobility. Under the deep mantle conditions, diffusion (and related processes) likely occurs via an extrinsic mechanism where defect concentration is controlled by the chemical environment such as oxygen fugacity. In such a case, the concentration of defect is related to the oxygen fugacity and the defect formation free energy, G_f^*, as (e.g., Flynn, 1972; Karato, 2008),

$$c \propto f_{O2}^r \cdot \exp\left(-\frac{G_f^*}{RT}\right) \tag{A1}$$

where r is a non-dimensional parameter and the defect formation free energy is given by,

$$G_f^* = E_f^* + P \cdot V_f^* - T \cdot S_f^* \tag{A2}$$

where E_f^* is the energy change associated with the formation of a defect, V_f^* is the volume change associated with the formation of a defect, S_f^* is the change in the (vibrational) entropy associated with the formation of a defect.

Here I will examine the pressure dependence of defect formation free energy for a vacancy and an interstitial atom to examine how the dominant defect type may change under high-pressure conditions. The contribution from vibrational entropy to defect concentration is $\exp(\frac{S_f^*}{R})$, but for most defects, $\frac{S_f^*}{R} \approx 1$ (e.g., Flynn, 1972; Shewmon, 1989), so the influence of this term is small and will be ignored. Consequently, I will focus on $H_f^* = E_f + P \cdot V_f$.

Typical point defects are vacancies and interstitial atoms. In most of oxides, commonly observed point defects at ambient temperatures are vacancies (e.g., Ando, 1989). This is because the formation of interstitial atoms requires a large excess energy compared to the formation of vacancies, i.e., E_f^* for a vacancy is smaller than E_f^* for an interstitial atom. However, under high-pressure conditions, the contribution from $P \cdot V_f^*$ term becomes important and hence the dominant type of point defect may change from vacancies at low pressures to interstitial atoms at high pressures. To see this point, let us take typical values of volume changes upon defect formation, 10×10^{-6} m³/mol. For this value, $P \cdot V_f^*$ term is =1000 kJ/mol (at P = 1 TPa) and is larger than a typical defect formation energies ($E_f^* \sim$ 100–300 kJ/mol, e.g., Flynn, 1972). Consequently, a difference in formation volume is expected to play an important role in controlling the dominant type of point defects under high-pressure conditions. Because the formation volume (the volume change upon the formation of a defect) for an interstitial atom is smaller than that for a vacancy, an interstitial atom will dominate under high-pressure conditions.

To explore this possibility, I use a simple model of a crystal with the *fcc* structure where the inter-atomic potential is represented by the Morse-potential acting only between the nearest neighbor atoms i.e.,

$$\phi(r) = \varepsilon\left[\exp\left\{-2\frac{r-r_0}{\rho}\right\} - 2\exp\left\{-\frac{r-r_0}{\rho}\right\}\right] \tag{A3}$$

where r is the inter-atomic distance, r_0 is the inter-atomic distance at P = 0, $-\varepsilon$ is the minimum energy (energy at $r = r_0$), and ρ is a parameter that is related to the shape (stiffness) of the potential (Fig. A1). In the following, I will use $t \equiv \frac{r_0}{\rho}$ to characterize the stiffness of the potential (when pressure is changed, t is defined in terms of inter-atomic distance at P = 0). This parameter is related to the pressure dependence of bulk modulus as $(\frac{\partial K}{\partial P})_0 = t + 1$.

I consider two types of point defects, namely a vacancy and an interstitial atom. When one forms a defect (such as a vacancy or an interstitial atom), one needs to change chemical bonding as well as the volume of a crystal. Also, when a defect is introduced in a crystal, a source of extra force is introduced at the defect site, and consequently the positions of other atoms move from the previous equilibrium positions. By this process, the enthalpy of a crystal will change (relaxation enthalpy). The calculation of enthalpy of formation of a crystalline defect was made in two steps. First, I calculate the enthalpy needed to form a defect when all other atoms remain their original positions. The enthalpy change for this first step corresponds to non-equilibrium state because due to the formation of
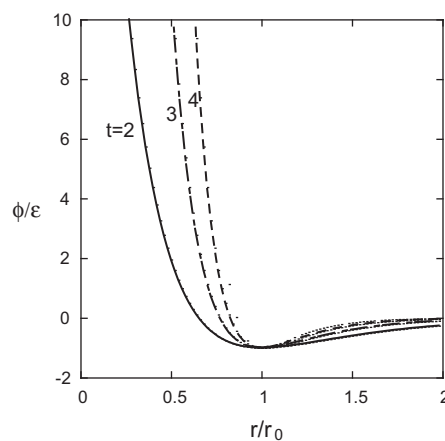

Fig. A1. The inter-atomic potential used in this study, r is the inter-atomic distance, and r_0 is the inter-atomic distance at P = 0. $t = r_0/\rho$ represents the "stiffness" of the potential.

a defect, excess force act on other atoms. Second step is to calculate the enthalpy change caused by the displacement of atoms caused by a defect. Consequently, the total free enthalpy change associated with the formation of a defect is given by,

$$H_f^* = H_{fI}^* + H_{fII}^* \tag{A4}$$

where H_{fI}^* is the enthalpy change necessary to create a defect without changing the positions of other atoms, and H_{fII}^* is the enthalpy change due to the displacement of all other atoms respectively (relaxation enthalpy). Both H_{fI}^* and H_{fII}^* have a $P \cdot \Delta V$ term related to the volume change, ΔV (ΔV: the volume change associated with the formation of a defect).

The calculation of H_{fII}^* was made explicitly without approximation for the atoms next to the defect, but the harmonic approximation was applied to atoms farther away and the lattice calculation in the far field was made using the Fourier transform following the method of Kanzaki (1957). This is due to the fact that atomic displacement of nearest neighbor atoms is large (∼10–20% of lattice spacing), whereas the atomic displacement becomes much smaller (less than a few %) from the second nearest neighbor and beyond. This method allows one to calculate the relaxation enthalpy using an infinite number of atoms (we assume the periodic boundary conditions) and the formation energy was calculated through the calculation in the wave-number space over the first Brillouin zone.

The free enthalpies of formation of a vacancy and an interstitial atom depend differently on the inter-atomic potential and pressure. The formation energy of an interstitial atom is highly sensitive to the nature of inter-atomic potential: the stiffer is the potential, the higher is the energy of formation of an interstitial atom (Fig. A2). The difference in formation energy (at zero pressure) does not change with pressure very much. However, because of the contribution of the $P \cdot \Delta V$ term, the formation free energy of a vacancy increases with pressure more rapidly than that of an interstitial atom. Consequently, there is a critical pressure at which the formation free energy of an interstitial atom becomes smaller than that of a vacancy. This critical pressure is sensitive to the nature of inter-atomic potential and the critical pressure increases with the stiffness of the potential. For a very weak potential ($t = 2$), interstitial mechanism always dominates whereas for a stiff potential, vacancy mechanism dominates for a broad range of pressure.
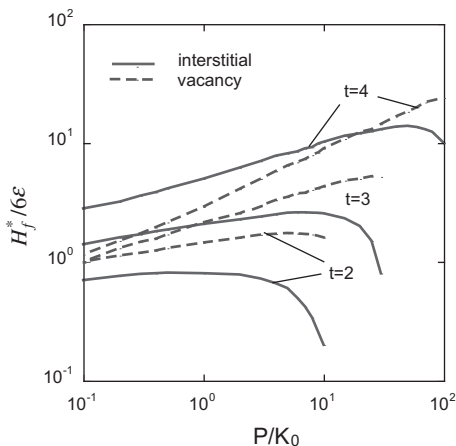

Fig. A2. The normalized pressure, P/K_0 (P: pressure, K_0: zero pressure bulk modulus), versus normalized free energy of formation ($H_f^*/6\varepsilon$) of vacancies and interstitial atoms for various values of stiffness parameter (reproduced from Karato (1978)). The stiffness parameter t is related to $\left(\frac{\partial K}{\partial P}\right)_{P=0}$ as $\left(\frac{\partial K}{\partial P}\right)_0 = t + 1$, and for $\left(\frac{\partial K}{\partial P}\right)_{P=0} = 4$ ($t = 3$), the transition pressure is ∼$0.8K_0$, but the transition pressure is highly sensitive to the stiffness and other features of inter-atomic potential.

References

Ammann, M.W. et al., 2010. First-principles constraints on diffusion in lower-mantle minerals and a weak D″ layer. Nature 465, 462–465.

Ando, K., 1989. Self-diffusion in oxides. In: Karato, S., Toriumi, M. (Eds.), Rheology of Solids and of the Earth. Oxford University Press, Oxford, pp. 57–82.

Flynn, C.P., 1972. Point Defects and Diffusion. Oxford University Press, Oxford.

Franssen, R.C.M.W., 1994. The rheology of synthetic rocksalt in uniaxial compression. Tectonophysics 233, 1–40.

Frost, H.J., Ashby, M.F., 1982. Deformation Mechanism Maps. Pergamon Press, Oxford.

Gaidos, E. et al., 2010. Thermodynamic limit on magnetodynamos in rocky exoplanets. Astrophys. J. 718, 596–609.

Goldreich, P., Soter, S., 1966. Q in the Solar System. Icarus 5, 375–389.

Gramsch, S.A. et al., 2003. Structure, metal–insulator transitions, and magnetic properties of FeO at high pressures. Am. Mineral. 88, 257–261.

Grocholski, B. et al., 2010. Stability of hte MgSiO₃ analog NaMgF₃ and its implication for mantle structure in super-Earths. Geophys. Res. Lett. 37. doi:10.1029/2010GL043645.

Handy, M.R., 1994. Flow laws for rocks containing two non-linear viscous phases: A phenomenological approach. J. Struct. Geol. 16, 287–301.

Heard, H.C., Kirby, S.H., 1981. Activation volume for steady-state creep in polycrystalline CsCl: cesium chloride structure. In: Carter, N.L. et al. (Eds.), Mechanical Behavior of Crustal Rocks. American Geophysical Union, Washington, DC, pp. 83–91.

Howard, A.W. et al., 2010. The occurence and mass distribution of close-in super-Earths, Neptunes, and Jupiters. Science 330, 653–655.

Ita, J., Cohen, R.E., 1997. Effects of pressure on diffusion and vacancy formation in MgO from nonempirical free-energy integration. Phys. Rev. Lett. 79, 3198–3201.

Ito, Y., Toriumi, M., 2007. Pressure effect on self-diffusion in periclase (MgO) by molecular dynamics. J. Geophys. Res. 112. doi:10.1029/2005JB003685.

Kanzaki, H., 1957. Point defects in face-centred cubic lattice-I. Distortion around defects. J. Phys. Chem. Solids 2, 24–36.

Karato, S., 1978. The concentration minimum of point defects under high pressures and the viscosity of the lower mantle. Programme and abstracts. Seismol. Soc. Jpn. 1, 216.

Karato, S., 1981. Pressure dependence of diffusion in ionic solids. Phys. Earth Planet. Int. 25, 38–51.

Karato, S., 1989. Plasticity-crystal structure systematics in dense oxides and its implications for creep strength of the Earth's deep interior: A preliminary result. Phys. Earth Planet. Int. 55, 234–240.

Karato, S., 2008. Deformation of Earth Materials: Introduction to the Rheology of the Solid Earth. Cambridge University Press, Cambridge.

Karato, S., 2010. The influence of anisotropic diffusion on the high-temperature creep of a polycrystalline aggregate. Phys. Earth Planet. Int. 183, 468–472.

Karki, B.B. et al., 1997. Structure and elasticity of MgO at high pressure. Am. Mineral. 82, 635–639.

Keyes, R.W., 1963. Continuum models of the effect of pressure on activated processes. In: Paul, W., Warschauer, D.M. (Eds.), Solids under Pressure. McGraw-Hill, New York, pp. 71–91.

Kite, E.S. et al., 2009. Geodynamics and rate of volcanism on massive Earth-like planets. Astrophys. J. 700, 1732–1749.

Knittle, E., Jeanloz, R., 1986. High-pressure metallization of FeO and implications for the Earth's core. Geophys. Res. Lett. 13, 1541–1544.

Landau, L.D., Lifshitz, E.M., 1964. Statistical Physics. Pergamon Press.

Lin, D.N.C. et al., 1996. Orbital migration of the planetary companion of 51 Pegasi to its present location. Nature 380, 606–607.

Meade, C., Jeanloz, R., 1988. Yield strength of the B1 and B2 phases of NaCl. J. Geophys. Res. 93, 3270–3274.

Merkel, S. et al., 2007. Deformation of (Mg, Fe)SiO₃ post-perovskite and D″ anisotropy. Science 316, 1729–1732.

Miyagi, L. et al., 2008. Deformation and texture development in CaIrO post-perovskite phase up to 6 GPa and 1300 K. Earth Planet. Sci. Lett. 268, 515–525.

Mott, N.F., 1968. Metal–insulator transition. Rev. Mod. Phys. 40, 677–683.

Nellis, W.J., 2010. Al₂O₃ as a metallic glass at 300 GPa. Phys. Rev., B82. doi:10.1103/PhysRevB.82.092101.

Oganov, A.R. et al., 2003. Ab initio lattice dynamics and structural stability of MgO. J. Chem. Phys. 118, 10174–10182.

O'Neill, C. et al., 2007. Conditions for the onset of plate tectonics on terrestrial planets and moons. Earth Planet. Sci. Lett. 261, 20–32.

Van Orman, J.A. et al., 2003. Diffusion in MgO at high pressure: constraints on deformation mechanisms and chemical transport at the core–mantle boundary. Geophys. Res. Lett. 30. doi:10.1029/2002GL016343.

Papuc, A.M., Davies, G.F., 2008. The internal activity and thermal evolution of Earth-like planets. Icarus 195, 447–458.

Peale, S.J., Cassen, P., 1978. Contribution of tidal dissipation to lunar thermal history. Icarus 36, 245–269.

Poirier, J.-P., Liebermann, R.C., 1984. On the activation volume for creep and its variation with depth in the Earth's lower mantle. Phys. Earth Planet. Int. 35, 283–293.

Ringwood, A.E., 1975. Composition and Structure of the Earth's Mantle. McGraw-Hill, New York.

Ross, M., Schubert, G., 1986. Tidal dissipation in a viscoelastic planet. J. Geophys. Res. 91, D447–D453.

Rowell, D.K., Sanger, M.J.L., 1981. Calculations of intrinsic defect energies in the alkali halides. J. Phys. Condens. Matter 14b, 2909–2921.

Sammis, C.G. et al., 1981. A critical assessment of estimation methods for activation volume. J. Geophys. Res. 86, 10707–10718.

Schubert, G. et al., 2001. Mantle Convection in the Earth and Planets. Cambridge University Press, Cambridge.

Sherby, O.D. et al., 1970. Calculation of activation volumes for self-diffusion and creep at high temperatures. J. Appl. Phys. 41, 3961–3968.

Shewmon, P.G., 1989. Diffusion in Solids. The Minerals, Metals & Materials Society, Warrendale, PA.

Sotin, C. et al., 2007. Mass–radius curve for extrasolar Earth-like planets and ocean planets. Icarus 191, 337–351.

Stauffer, D., Aharony, A., 1992. Introduction to Percolation Theory. Taylor and Francis, London.

Tachinami, C., et al., 2010. Thermal evolution and lifetime of intrinsic magnetic fields of super Earths in habitable zones. Astrophys. J., in press.

Todo, S. et al., 2001. Metallization of magnetite (FeO) under high pressure. J. Appl. Phys. 89, 7347–7349.

Tozer, D.C., 1972. The present thermal state of the terrestrial planets. Phys. Earth Planet. Int. 6, 182–197.

Umemoto, K. et al., 2006. Dissociation of MgSiO in the cores of gas giant and terrestrial exoplanets. Science 311, 983–986.

Valencia, D., O'Connell, R.J., 2009. Convection scaling and subduction on Earth and super-Earth. Earth Planet. Sci. Lett. 286, 492–502.

Valencia, D. et al., 2006. Internal structure of massive terrestrial planets. Icarus 181, 545–554.

Valencia, D. et al., 2007a. Detailed models of super-Earths: How well can we infer bulk properties? Astrophys. J. 665, 1413–1420.

Valencia, D. et al., 2007b. Radius and structure models of the first super-Earth planet. Astrophys. J. 656, 545–551.

Yamazaki, D., Karato, S., 2001. Some mineral physics constraints on the rheology and geothermal structure of Earth's lower mantle. Am. Mineral. 86, 385–391.

Yamazaki, D. et al., 2006. Origin of seismic anisotropy in the D" layer inferred from shear deformation experiments on post-perovskite phase. Earth Planet. Sci. Lett. 252, 372–378.